Glass formation and crystallization of a simple monatomic liquid

Tomoko Mizuguchi* and Takashi Odagaki†
Department of Physics, Kyushu University, Fukuoka 812-8581, Japan
(Received 16 March 2009; published 11 May 2009)

A simple monatomic system in two dimensions with a double-well interaction potential is investigated in a wide range of temperatures by molecular-dynamics simulation. The system is melted and equilibrated well above the melting temperature, and then it is quenched to a temperature 88% below the melting temperature at several cooling rates to produce an amorphous state. Various thermodynamic quantities are measured as functions of temperature while the system is heated at a constant rate. The glass transition is observed with a sudden increase in the energy and the glass transition temperature is shown to be an increasing function of the cooling rate in the preparation process of the amorphous state. In a relatively high-temperature region, the system gradually transforms into crystals, and the time-temperature-transformation curve shows a typical nose shape. It is found that the transformation time to a crystalline state is the shortest at a temperature 14–15 % below the melting temperature and that at sufficiently low temperatures the system does not transform into a crystalline state within an observation time in our simulation. This indicates that a long-lived glassy state is realized.

DOI: 10.1103/PhysRevE.79.051501 PACS number(s): 64.70.Q−, 64.70.P−, 68.18.Jk, 05.10.−a

I. INTRODUCTION

For a long time, a lot of studies have been made in understanding the glass transition by experimental, theoretical, and computational methods [1–3]. One of the difficulties in understanding the glass transition arises from the fact that almost all glass-forming materials consist of many constituents. Even in a computer simulation, more than two components are needed in order to avoid crystallization [4–6]. The problem in a simple monatomic system is that crystallization occurs in a relatively short time. Since a long-time simulation is needed to investigate the slow dynamics around the glass transition point, a binary mixture is usually investigated.

In order to avoid the crystallization of simple liquids in simulations, the Dzugutov potential was proposed [7]. The Dzugutov potential has an additional maximum to the Lennard-Jones (LJ) potential at a range typical of the next-nearest-neighbor coordination distance in close-packed crystals, which suppresses the crystallization. Indeed, the system remains in a metastable supercooled state for a long time and shows some characteristic behaviors of glass-forming liquids [7,8]. However, it turned out to form a dodecagonal quasicrystal by freezing in a subsequent simulation [9].

In fact, features of a glass formation are incompletely understood even for the simplest system, so it is attractive to carry out the study using a sophisticated monatomic system. In multicomponent systems, the relaxation involves both the topological and the chemical orderings. A spherically interacting one-component model system provides an opportunity for separating these contributions and enables us to explore the topological effect on the relaxation dynamics around the glass transition point. It is useful for comparison with theories, since most theoretical works [10–15] assume a simple system.

For the purpose of studying the glass formation of a simple liquid, we employ a monatomic model system in two dimensions with a double-well interaction potential, the Lennard-Jones-Gauss (LJG) potential [16,17]. In a previous paper [18], we showed that the LJG system can be vitrified in two dimensions and the glassy state at low temperatures is stable for a fairly long time in spite of a simple monatomic potential. In addition, for three-dimensional (3D) systems the glass-forming ability of the LJG system has been tested and discussed [19].

In this paper, we show the further study of the glassy feature in this LJG system. In addition, we investigate the aging-induced crystallization with molecular-dynamics (MD) simulations. In general simulations, the model system is chosen to realize a stable supercooled liquid state, while the crystallization is highly suppressed. Therefore, correct descriptions of the relaxation process of the glass-forming liquids are still not really understood, and we focus attention on this point.

This paper is organized as follows. In Sec. II, we explain our model and methods of MD simulation in detail. We present the evidence of vitrification of this system in Sec. III A and we show the results of the crystallization process in Sec. III B. We close with concluding remarks in Sec. IV.

II. MODEL POTENTIAL

We consider a system of atoms which interact isotropically through the LJG potential

$$V(r) = \epsilon_0 \left\{ \left(\frac{r_0}{r} \right)^{12} - 2 \left(\frac{r_0}{r} \right)^{6} \right\} - \epsilon \exp\left(- \frac{(r - r_G)^2}{2\sigma^2} \right). \quad (1)$$

The LJG potential consists of the LJ potential and a pocket represented by the Gaussian function. It forms a double-well potential for most values of the parameters with the second well at position r_G, of depth ϵ and width σ. This kind of effective potential is known to exist in metals. The general

*t.mizuguchi@cmt.phys.kyushu-u.ac.jp
†Also at Division of Science, School of Science and Engineering, Tokyo Denki University, Hatoyama, Hikigun, Saitama 350-0394, Japan.

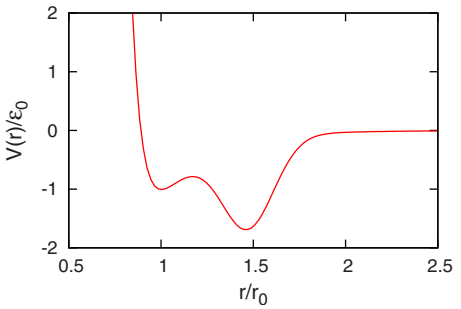

FIG. 1. (Color online) The LJG potential for the parameters $r_G=1.47r_0$, $\epsilon=1.5\epsilon_0$, and $\sigma^2=0.02r_0^2$.

form of pair potentials in metals consists of a strongly repulsive core plus a decaying oscillatory term [20]. The LJG potential can be understood as such an oscillatory potential, cut off after the second minimum. This potential was proposed for the self-assembly of two-dimensional monatomic complex crystals and quasicrystals [16]. It has also been used as a model of liquid water [21] and as a potential for stabilization of a given structure [22,23]. We have found stable glassy states at some parameter regions.

Here, we fix the parameters $r_G=1.47r_0$, $\epsilon=1.5\epsilon_0$, and $\sigma^2=0.02r_0^2$. Figure 1 shows the LJG potential with these parameters. This set of parameters produces the pentagon-triangle phase in the ground state [17]. The unit of length, energy, and time in the present simulation are r_0, ϵ_0, and $\tau \equiv (mr_0^2/\epsilon_0)^{1/2}$, respectively.

We perform a constant-volume MD simulation for 2500 atoms on two-dimensional space with periodic boundary conditions (PBCs). The size of the simulation box is chosen so that the number density becomes $\rho=1.0$. We employ a Verlet algorithm with time mesh of 0.01τ.

III. RESULTS AND DISCUSSIONS

A. Glass transition

In order to determine the glass transition point, we follow the procedure employed in the thermodynamic measurement [24]. Namely, we quench the system much below the melting temperature T_m^*, and anneal it for some time. Then we heat the system at a constant rate and measure the energy of the system. The glass transition temperature T_g^* is identified by a change in the slope of E vs T graph.

We prepare an equilibrium liquid state as the initial condition at $T^* \equiv k_BT/\epsilon_0=2.2$, which is above $T_m^*=0.43$, and then cool the system down to a target temperature with the velocity scaling. When the target temperature is close to but below T_m^*, the system transforms into a crystalline state after some time. However, the target temperature is well below T_m^*; the system remains in the amorphous state even for a long-time run. Figure 2 shows tiling structures in real space and diffraction images of a glass and crystal after $(3.5\times10^5)\tau$. We determined tilings by drawing a line between the particles within a cutoff radius, where the cutoff radius is chosen as the first minimum of the radial-distribution function of the system. Triangle and pentagon tiles are essential for stable

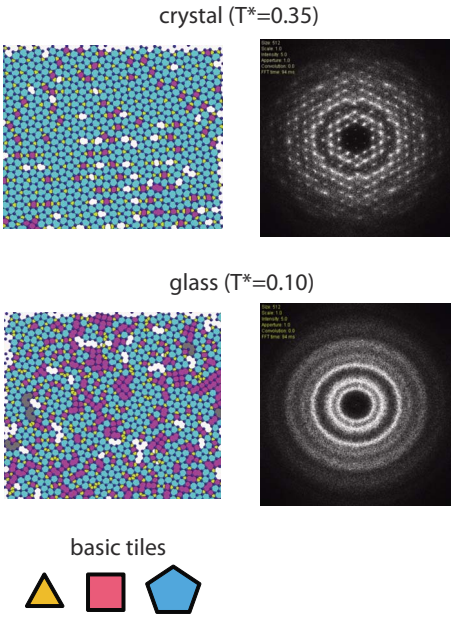

FIG. 2. (Color online) Tiling structures in real space and diffraction images of a glass and crystal after a long run. Upper panels are the structure of crystal at $T^*=0.35$ and lower ones are that of glass at $T^*=0.10$. Left panels show the tiling structures in real space. These are constructed by basic tiles. Right panels show the diffraction images.

structures of this system. In the glassy state, no periodic order is observed.

Figure 3 shows the radial distribution function of a glassy state. The position of the first peak is at 0.93 and the second peak is at 1.50. The position of the second peak approximately coincides with the second minimum of LJG potential. The position of the first peak is slightly inner than that of the first minimum of the potential. Here, we consider a regular pentagon, and if the distance between second nearest particles has the value of 1.47, the distance between nearest particles becomes about 0.91. This means the potential used in this study favors a pentagonal local order especially because of the position of the second minimum. This pentagonal local order is essential for the stability of the glass in this system. The third and fourth peaks represent the existence of the local structure consisting of one pentagon and one triangle (see Fig. 3). These tiles share an edge and make an ordered arrangement in a crystalline state, while it randomly

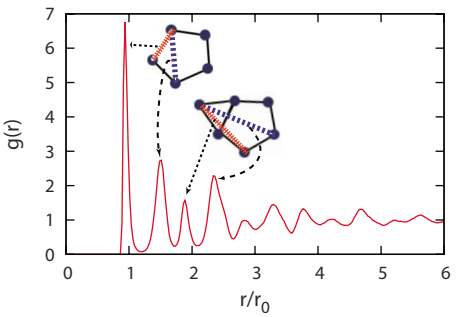

FIG. 3. (Color online) The radial distribution function of a glassy state at $T^*=0.1$ and local structures.

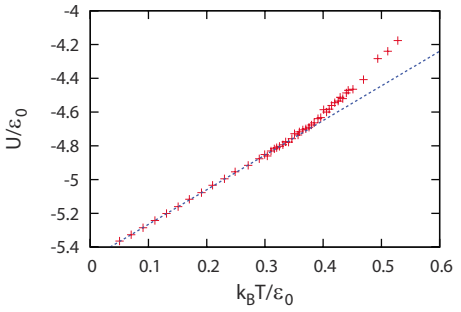

FIG. 4. (Color online) The temperature dependence of the total energy in a heating process from a glassy state. If the system can be described only by the term of lattice vibration, plots are supposed to lie on the line in above figure.

spreads out all over the system in a glassy state (see Fig. 2).

Figure 4 shows the change in the total energy in a heating process from a glassy state at $T^*=0.05$ prepared with cooling rate $\gamma_q=10^{-2}\epsilon_0/k_B\tau$. The heating rate from a glassy state is $\gamma_h=10^{-3}\epsilon_0/k_B\tau$. The slope of the black line in Fig. 4 is about 2, which represents the energy change due to the vibration. Simulation data lie on the black line at lower temperatures, which indicates that the specific heat is determined by the vibrational motion of atoms. However, plots start to deviate from the line at $T^*\sim 0.38$, which is below the melting temperature, so that an additional effect appears in addition to that of vibration. Crystallization does not occur in this heating process, which is confirmed by the static structure factor. That means the system transforms from a glassy state into a supercooled state as the temperature is increased. If we take $\gamma_h=10^{-4}\epsilon_0/k_B\tau$ as the heating rate, the sign of crystallization appears in the heating process, so we cannot decide the glass transition point with confidence. Thus, we conclude that the glass transition temperature is $T^*\sim 0.38$ in this sample. We perform the heating simulation starting from glassy samples prepared by different cooling rates and determine T_g^* for each sample. Figure 5 shows the cooling rate dependence of T_g^*. We find that T_g^* is an increasing function of the cooling rate, which is consistent with experiments [25].

B. Time-temperature-transformation diagram

In this section, we investigate the structural transformation into a crystal in the real space. We first prepared an equilibrium liquid state at $T^*=0.4$ above the melting temperature $T_m^*\simeq 0.34$. Then, we quenched the system to several target temperatures instantaneously. After the quenching, we control the system temperature using a Nosé-Hoover thermostat and allowed it to relax at this temperature. We employ the instantaneous cooling in order to avoid any nucleation during the cooling process which may hinder proper comparison of the crystallization process. The simulation cell is made large enough so that the system feels zero pressure at all times. Under the free boundary conditions (FBCs), particles on the surface can easily move, so rearrangement of particles can frequently occur, compared with periodic boundary conditions. Since crystallization proceeds more drastically, we can determine easily the time when the system crystallizes. The number of atoms in the system is $N=1024$ and the leapfrog algorithm is employed.

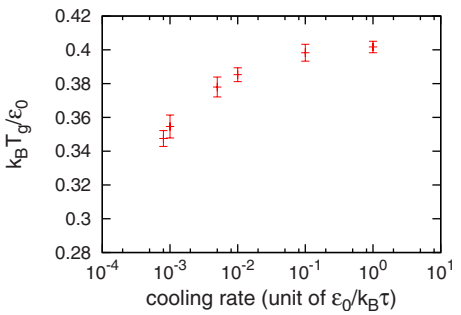

FIG. 5. (Color online) The cooling rate dependence of T_g^*.

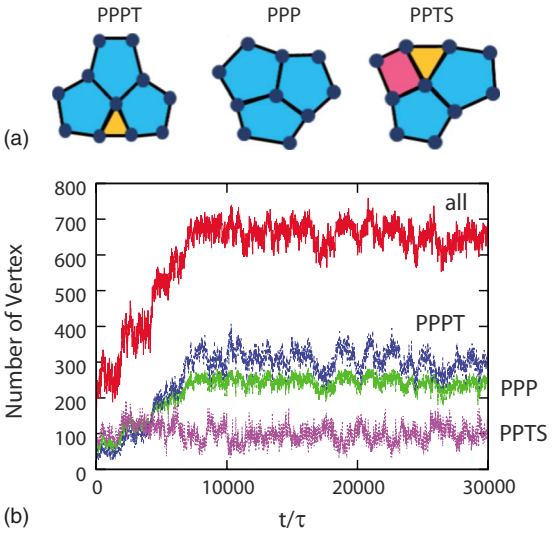

FIG. 6. (Color online) (a) Three characteristic tiling structures. (b) The time dependence of the number of characteristic tiling structures. The curve (all) represents the number of atoms surrounded by any of the pentagon, triangle, or square tiles. The curves PPPT, PPP, and PPTS correspond to the structures shown in (a).

We checked the time needed for crystallization at each temperature and determined a time-temperature-transformation (TTT) diagram. In order to determine the crystallization time, we focus on the formation of three characteristic tiling structures, PPPT, PPP, and PPTS, which consist of pentagons, squares, and triangles shown in Fig. 6(a). Figure 6(b) shows the time dependence of the number of atoms whose surroundings can be identified as the three characteristic tiling structures. The curve (all) shows the number of particles surrounded by any of the pentagons, triangles or squares. This value is related to the potential energy and becomes constant when the system reaches a crystalline state. At relatively high temperatures, the transition from the supercooled liquid to a crystal is rather sharp and we can determine the crystallization time without ambiguity. As the temperature is reduced, the transformation tends to be less sharp, and we determined the transition time by observing diffraction patterns as well as the evolution of tilings.

Figure 7 shows the crystallization time as a function of temperature, which is known as a TTT diagram. This diagram indicates that the crystallization time becomes the

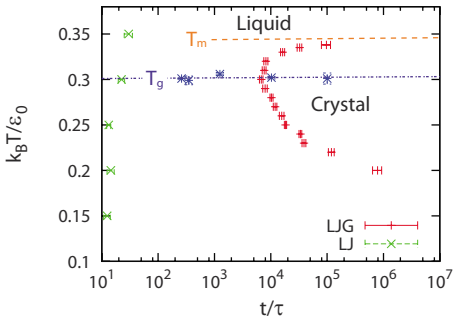

FIG. 7. (Color online) The time-temperature-transformation diagram for monatomic LJ and LJG liquids.

shortest at $\sim 0.86T_m^*$ and it is longer than $10^7\tau$ at $0.5T_m^*$. If one uses the values of m, r_0, and ϵ_0 relevant for the LJ potential of Ar, this time of $10^7\tau$ corresponds to 10 μs. The glass transition temperature T_g^* shown in Fig. 7 is determined under the following condition. First, we prepared a glassy sample by instantaneous cooling to $0.15T_m^*$. After that, the sample was annealed at this temperature with different annealing times: 10τ, $10^2\tau$, $10^3\tau$, $10^4\tau$, and $10^5\tau$. We used these five samples as initial states for determination of glass transition. The temperature was increased from these initial states by $10^{-3}\epsilon_0/k_B$ a step and the energy was determined by its average for 1τ period at each temperature step. Finally, we determined T_g^* by a sudden increase in E vs T graph. We found that T_g^* does not depend on the waiting time and is located at the temperature which a crystallization time is the shortest.

For comparison, the results for a monatomic LJ system are also plotted in Fig. 7. Consequently, the LJG system has a much longer crystallization time than the LJ system, and we can clearly see the temperature dependence of the TTT diagram in the LJG system. It shows a typical nose shape, which has been observed by experiments for various glass-forming materials [26–28]. A similar TTT diagram is also found by MD simulations with some empirical potentials for metal [29,30]. Our system has a much longer crystallization time than that reported in these papers in spite of the simpler shape of our interatomic potential.

A LJ liquid rapidly transforms into the triangle lattice at a few thousand MD steps. At low temperatures, particles condense into some clusters which are separated by some voids, and then such voids are eliminated gradually. On the other hand, at high temperatures, the system can transform in such a way that voids do not appear because particles can move more freely. This is the reason that the crystallization time in a LJ system becomes slightly longer at higher temperatures.

Figure 8 shows results for the relaxation time dependence of potential energy at temperatures from 0.338 to 0.33 and from 0.23 to 0.20. It can be found from Fig. 8(a) that the system at temperatures very close to $T_m^*(=0.34)$ behaves as if it is an equilibrium liquid state for a while, and it drastically transforms into a crystalline state by nucleation. The crystallization time in this temperature region is distributed because it depends on whether nucleation occurs or not by chance. Figure 9 shows one example of the process of nucleation and growth at temperatures close to T_m^*. In Fig. 9, the nucleation

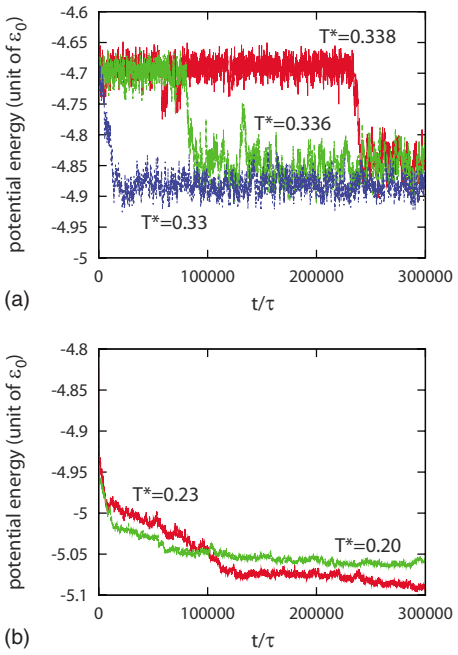

FIG. 8. (Color online) Time dependence of potential energy at several temperatures. (a) shows the region close to T_m^*, $0.33 \leq T^* \leq 0.338$. (b) shows the region at low temperatures, $0.20 \leq T^* \leq 0.23$.

(a) occurs in the inner part, and (b) grows rapidly. However in a while, (c) the order is destroyed from the outer side. Since particles, especially on the surface, can move around rather freely, rearrangement can easily occur. Therefore, the system can remove defects and (d) eventually reaches a per-

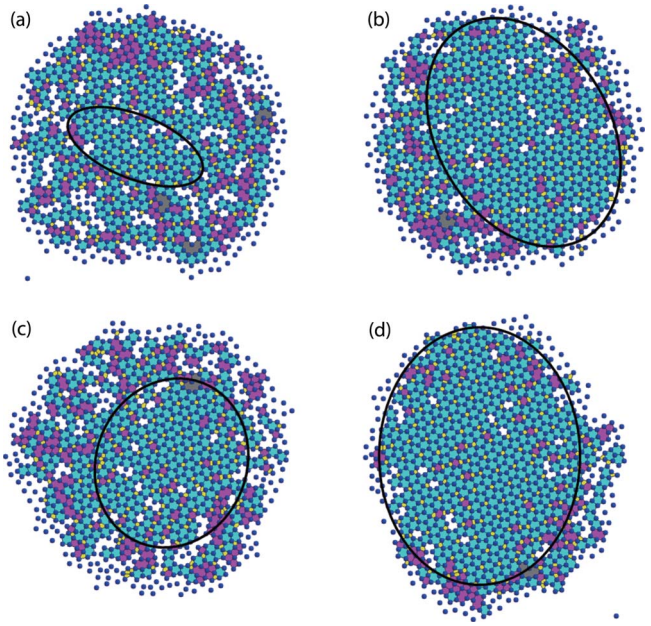

FIG. 9. (Color online) The process of nucleation and growth at a temperature close to T_m^*. (a) The nucleation occurs in the center. (b) The nucleation grows rapidly. (c) A part of crystalline phase is destroyed and rearrangement occurs. (d) Eventually, the system becomes an almost perfect crystal.

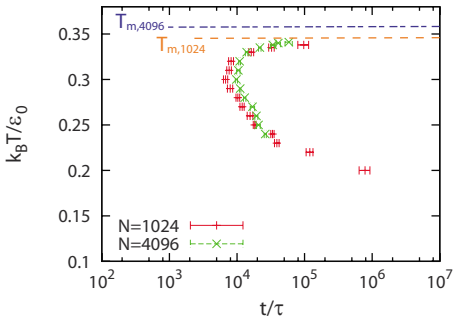

FIG. 10. (Color online) The system-size dependence of the time-temperature-transformation diagram for monatomic LJG liquids. The numbers of particles in each system are 1024 and 4096. The temperature range in $N=4096$ system is from 0.24 to 0.341.

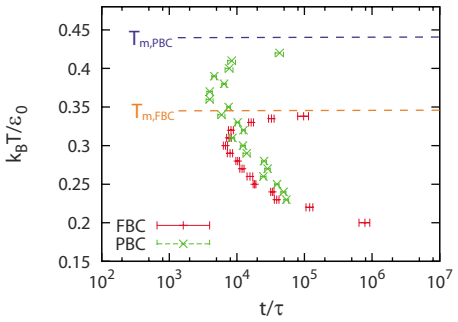

FIG. 11. (Color online) The boundary condition dependence of the time-temperature-transformation diagram for monatomic LJG liquids.

fect crystal. In Fig. 8(b), the potential energy at a low temperature shows a higher value for long time scales compared with those at higher temperatures. It indicates that the system at sufficiently low temperatures remains in a metastable state for a long time.

Figure 10 shows the system-size dependence of TTT diagram. The numbers of particles in each system are $N=1024$ and 4096. In both systems, a longer time is needed for crystallization near T_m^*, and the temperature which has the shortest crystallization time is almost the same. T_m^* in a larger system is higher than that in a smaller system. This tendency agrees with the size dependence of T_m^* found in confined systems [31]. We also find that the shortest time in a large system becomes longer than that of small systems. It is because in a large system, a much longer time is needed for the spread of crystalline phase to the whole system. However, at lower temperatures, the growth of the crystallization time is suppressed in a large system. The reason of this result is that the state is different between two systems at the time when the system is assumed to have crystallized. At this time, many samples in the $N=4096$ system are a polycrystalline state which has more than two domains. On the other hand, the $N=1024$ system has less domains and sometimes one domain spreads to the whole system. If we determine the crystallization time when the system has one or two domains, a large system will take a longer time to crystallize.

We also investigated the crystallization time under PBCs. The boundary condition dependence of the TTT diagram is shown in Fig. 11. The number of particles is 1024 in both systems. It is difficult to determine the crystallization time clearly under PBCs in the same way as under FBCs. In both systems, first nucleation occurs at almost same time. The difference appears in a subsequent process. In a system under FBCs, if the nucleus starts to grow, a crystal phase spreads rapidly to the entire system. It is more difficult for the nucleus to grow under PBCs and a perfect crystal cannot be obtained unlike under FBCs. We determine the crystallization time under PBCs by the potential energy, which remains nearly constant after a long time scale (i.e., the crystallization time). The definition of crystallization time is different from one in FBCs system. Under FBCs, we define the crystallization time as when the number of characteristic tiling structures becomes nearly constant. The similarities between these two systems are that the crystallization time becomes longer at temperatures close to T_m^* and it is the shortest at a temperature 15% below T_m^*. The difference appears in a behavior at low temperatures. The growth of the crystallization time in PBCs system is suppressed compared to that of FBCs system. Also in this case, the state is different between two systems at the time when the system is assumed to have crystallized. A crystalline state in PBCs system is less perfect than that of FBCs system. It is more difficult in PBCs system to get a perfect crystal because of boundary constraint.

IV. CONCLUSIONS

We presented strong evidence of vitrification of a simple monatomic liquid in two dimensions by an adequate choice of LJG parameters. We have shown that the glassy state can survive a fairly long time at low temperatures and the glass transition temperature is an increasing function of the cooling rate in the preparation process of the amorphous state. The Gaussian part of the LJG potential stabilizes the pentagonal configuration and packing of pentagons produces frustration in crystallization. Two competing length scales and the local structure made by them can have a great impact on the degree of disorder in the system, which leads to suppress crystallization. It has also been shown that in 3D systems [19], the glassy state can be formed if the LJG potential has appropriate parameters favoring the formation of an icosahedral local order. The effect of this frustration with packing is the origin of the stability of the glassy state.

One of the features of this system is that the time needed for crystallization is sufficiently long. It enabled us to determine the TTT diagram of the simple system. It has a nose shape and the transformation time into crystal is the shortest at a temperature 14–15 % below T_m^*, which are independent of the system size and boundary conditions. Above the glass transition temperature, crystal nuclei rapidly spread to the whole system. Below T_g^*, the growth of crystal nuclei becomes slower as temperature is decreased, because rearrangement of atoms occurs less frequently.

This model will enable us to explore in greater detail the mechanism of nucleation and growth processes in the monatomic glass. The study in this direction will lead us to solve the problem about slow nucleation kinetics of glass-forming liquids. Due to simplicity of the model, one can use the LJG

system for further study of other phenomena related to the glass transition and for a detailed comparison with theories.

ACKNOWLEDGMENTS

We would like to thank Dr. Michael Engel of Stuttgart University for providing us the software on which most of the simulations and analysis for this work were carried out. This work was supported in part by the Grant-in-Aid for Scientific Research from the Ministry of Education, Culture, Sports, Science and Technology of Japan.

[1] C. A. Angell, K. L. Ngai, G. B. McKenna, P. F. McMillan, and S. W. Martin, J. Appl. Phys. **88**, 3113 (2000).
[2] R. Schilling, in *Collective Dynamics of Nonlinear and Disordered Systems*, edited by G. Radons, W. Just, and P. Haeussler (Springer, New York, 2003), pp. 171–202.
[3] W. Kob, J. Phys.: Condens. Matter **11**, R85 (1999).
[4] W. Kob and H.-C. Andersen, Phys. Rev. E **51**, 4626 (1995).
[5] W. Kob and H.-C. Andersen, Phys. Rev. E **52**, 4134 (1995).
[6] B. Bernu, J.-P. Hansen, Y. Hiwatari, and G. Pastore, Phys. Rev. A **36**, 4891 (1987).
[7] M. Dzugutov, Phys. Rev. A **46**, R2984 (1992).
[8] M. Dzugutov, J. Non-Cryst. Solids **156–158**, 173 (1993).
[9] M. Dzugutov, Phys. Rev. Lett. **70**, 2924 (1993).
[10] U. Bengtzelius, W. Götze, and A. Sjölander, J. Phys. C **17**, 5915 (1984).
[11] W. Götze, in *Liquids, Freezing and the Glass Transition*, edited by J.-P. Hansen, D. Levesque, and J. Zinn-Justin (North-Holland, Amsterdam, 1989).
[12] W. Götze, J. Phys.: Condens. Matter **11**, A1 (1999).
[13] T. Odagaki, Phys. Rev. Lett. **75**, 3701 (1995).
[14] T. Odagaki, T. Yoshidome, A. Koyama, and A. Yoshimori, J. Non-Cryst. Solids **352**, 4843 (2006).
[15] M. Mezard and G. Parisi, J. Chem. Phys. **111**, 1076 (1999).
[16] M. Engel and H.-R. Trebin, Phys. Rev. Lett. **98**, 225505 (2007).
[17] M. Engel and H.-R. Trebin, Z. Kristallogr. **223**, 721 (2008).
[18] T. Mizuguchi, T. Odagaki, M. Umezaki, T. Koumyou, and J. Matsui, in *Complex Systems*, edited by M. Tokuyama, I. Oppenheim, and H. Nishiyama, AIP Conf. Proc. No. 982 (AIP, New York, 2008), pp. 234–237.
[19] V. V. Hoang and T. Odagaki, Physica B **403**, 3910 (2008).
[20] I. Al-Lehyani, M. Widom, Y. Wang, N. Moghadam, G. M. Stocks, and J. A. Moriarty, Phys. Rev. B **64**, 075109 (2001).
[21] P. A. Netz, J. F. Raymundi, A. S. Camera, and M. C. Barbosa, Physica A **342**, 48 (2004).
[22] M. C. Rechtsman, F. H. Stillinger, and S. Torquato, Phys. Rev. E **73**, 011406 (2006).
[23] M. C. Rechtsman, F. H. Stillinger, and S. Torquato, Phys. Rev. E **74**, 021404 (2006).
[24] O. Yamamuro, I. Tsukushi, A. Lindqvist, S. Takahara, M. Ishikawa, and T. Matsuo, J. Phys. Chem. B **102**, 1605 (1998).
[25] M. Sugisaki, K. Adachi, H. Suga, and S. Seki, Bull. Chem. Soc. Jpn. **41**, 593 (1968).
[26] R. Busch, J. Schroers, and W. H. Wang, MRS Bull. **32**, 620 (2007).
[27] S. Mukherjee, J. Schroers, W. L. Johnson, and W. K. Rhim, Phys. Rev. Lett. **94**, 245501 (2005).
[28] H. Senapati, R. K. Kadiyala, and C. A. Angell, J. Phys. Chem. **95**, 7050 (1991).
[29] A. V. Evteev, A. T. Kosilov, E. V. Levchenko, and O. B. Logachev, J. Exp. Theor. Phys. **101**, 521 (2005).
[30] Y. Zhang, L. Wang, and W. Wang, J. Phys.: Condens. Matter **19**, 196106 (2007).
[31] C. L. Jackson and G. B. McKenna, J. Chem. Phys. **93**, 9002 (1990).